

Supporting Information for
Environmental Science and Technology

Assessing Aerobic Biotransformation of Hexachlorocyclohexane Isomers by Compound-Specific Isotope Analysis

Iris E. Schilling^{1,2}, Charlotte E. Bopp^{1,2}, Rup Lal³, Hans-Peter E. Kohler^{*,1,2}
and Thomas B. Hofstetter^{*,1,2}

¹Eawag, Swiss Federal Institute of Aquatic Science and Technology

²Institute of Biogeochemistry and Pollutant Dynamics (IBP), ETH Zürich

³Department of Zoology, University of Delhi

*Corresponding authors:

`hanspeter.kohler@eawag.ch` and

`thomas.hofstetter@eawag.ch`

phone +41 58 765 50 76, fax +41 58 765 50 28

26 Pages, 8 Figures, 6 Tables

Contents

S1 Chemicals	3
S1.1 Chemicals	3
S1.2 Stock solutions	3
S1.3 Isotopic standards	3
S2 Protein expression and purification	3
S3 Experimental setup and chemical analyses	5
S4 Data evaluation	5
S4.1 Conformational analysis	5
S4.2 Apparent kinetic isotope effects	7
S4.2.1 Dehydrochlorination by LinA2	9
S4.2.2 Hydrolytic dechlorination by LinB	10
S4.2.3 Calculation of ^2H -AKIE values associated with HCH dehydrochlorination by LinA2	11
S4.3 Interpretation of H isotope fractionation associated with α -HCH transformation by LinA2 and LinB	13
S4.3.1 α -HCH dehydrochlorination by LinA2	13
S4.3.2 Hydrolytic dechlorination of α -HCH by LinB	15
S4.3.3 Matlab Scripts	17
S5 Additional Data	20
S5.1 Chemical structures of substrates and products	20
S5.2 Survey of investigations of aerobic HCH biodegradation and -transformation with compound-specific isotope analysis	22
S5.3 Reaction rate constants and catalytic efficiencies	23
S5.4 Pentachlorocyclohexenes from α -HCH	24
S5.5 Additional data for the LinA2 catalyzed transformation of β -HCH	25
S5.6 Additional data for the LinB catalyzed transformation of β -HCH	25
S6 References	26

S1 Chemicals

Chemicals, stock solutions, and isotopic standards are largely identical to the materials used in our previous study by Schilling et al.¹⁷ and this information is reproduced here with minor modifications.

S1.1 Chemicals

1,2,3-Trichlorobenzene (1,2,3-TCB, purity of 99.9 %) and 1,2,4-TCB (99.4 %), sodium hydroxide, hydrochloric acid, LB broth, L-(+)-arabinose, chloramphenicol, sodium chloride, Trizma®-base, glycine, imidazole, ethanol, aluminum sulfate hexadecahydrate, coomassie brilliant blue G250, ortho-phosphoric acid (85%) were purchased from Fluka/Sigma-Aldrich. Sodium dihydrogen phosphate monohydrate, acetone, acetonitrile, *n*-hexane, ethyl acetate, patinal chromium powder from Merck. α -Hexachlorocyclohexane (α -HCH) (> 98%), β -HCH (> 98%), γ -HCH, 99 %), and δ -HCH (> 98%) were purchased from Maag. Ampicillin sodium salt was purchased from AppliChem. Hexachlorobenzene was purchased from Santa Cruz Biotechnology.

S1.2 Stock solutions

All chemicals for buffers and microbiological work were used as received. Buffer solutions for fast-protein liquid chromatography (FPLC) and experiments were prepared with nanopure water (18.2 M Ω -cm, Barnsted™ NANOpure™, Thermo Fisher Scientific) and the pH was adjusted to 7.5 with 5 mM or 0.5 mM sodium hydroxide (Sigma-Aldrich) or 1 mM hydrochloric acid (Fluka). Sodium dodecyl sulfate-polyacrylamide gel electrophoresis (SDS-PAGE) was run with Novex® tricine SDS sample buffer (2x), invitrogen NuPAGE® reducing agent (10x), and Novex® tricine SDS running buffer (all Thermo Fisher Scientific). Staining and destaining solutions were prepared according to Dyballa and Metzger⁵. We used precision plus protein™ Dual Color standard (Biorad) and peqGOLD protein marker IV (VWR) as a protein standard.

S1.3 Isotopic standards

Standard materials for C isotope analysis included γ -HCH ($\delta^{13}\text{C} = -26.7 \pm 0.1\text{‰}$), hexachlorobenzene standard 1 ($\delta^{13}\text{C} = -25.4 \pm 0.1\text{‰}$), and hexachlorobenzene standard 2 ($\delta^{13}\text{C} = -28.7 \pm 0.1\text{‰}$). $\delta^{13}\text{C}$ of γ -HCH and HCBs were determined with an elemental analyzer/IRMS. For H isotope analysis, we used hexadecane ($\delta^2\text{H} = -9.1 \pm 1.4\text{‰}$) and heptadecane ($\delta^2\text{H} = -117.9 \pm 2.3\text{‰}$) and both materials were purchased from Schimmelmann et al.¹⁸, Indiana University.

S2 Protein expression and purification

The protocols for expression and purification of LinA2 and LinB are reproduced here from a similar description for preparation of LinA1 and LinA2 by Schilling et al.¹⁷. For the expression of LinA2 and LinB from *Sphingobium indicum* B90A, *E. coli* BL21AI, an arabinose-inducible strain, was transformed with the plasmid vector pDEST17 encoding codon-optimized, synthetic

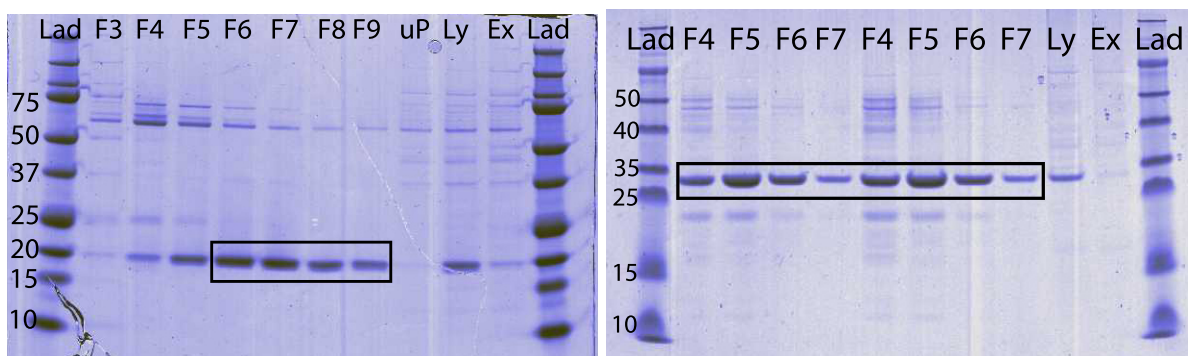


Figure S1 SDS Gels for LinA2 (left) and LinB (right) FPLC fraction purity analyses. The columns are marked as follows: Lad. – ladder, protein standard (in kDa), F – FPLC fraction number, uP – unbinding protein, Ly – lysate (1:100), Ex – extract (1:100). FPLC fractions of LinA2 and LinB used for further purification are marked with a black box. For LinB purification, two FPLC runs were performed per batch.

and 6x His-tagged *linA2* or *linB* as well as ampicillin resistance.¹ For enhanced folding of LinA2 the respective *E. coli* BL21AI was additionally transformed with pGro7 (Takara Bio Inc.), which encodes the chaperone protein groES-groEL and chloramphenicol resistance.

Cells transformed with pDEST17 with either *linA2* or *linB* were grown in LB at 37 °C with an antibiotic pressure of 450 μ M ampicillin and, for cells expressing LinA2, 10.5 μ M chloramphenicol additionally. At an OD₆₀₀ of 0.6, 2 g/L L-(+)-arabinose was added to induce the expression of the target enzyme, and the temperature was reduced to 30 °C. When the induced culture reached an OD₆₀₀ of > 1.8, we harvested the cells by centrifugation (10'000 rpm for 20 min at 4 °C), collected the cell pellets, and stored them at –20 °C.

To purify LinA2 and LinB from pelleted cells, 1 g of pelleted cells was suspended in 3 to 5 mL buffer (50 mM NaH₂PO₄ · H₂O, 300 mM NaCl, 10 mM imidazole) and exposed to ultrasonication (Sonoplus HD 3200 with MS73 needle, Bandelin electronic) under constant cooling on ice. We purified LinA2 and LinB by means of an ÄKTA FPLC system (GE Healthcare Life Science) on two separate Ni-NTA Superflow cartridges (5 mL, Qiagen) to avoid cross-contamination of the two enzymes. The proteins were eluted by applying an imidazole gradient (10 mM to 300 mM). The concentration of proteins was quantified spectrophotometrically with a NanoDrop ND-1000 device (Thermo Scientific) at a wavelength of 280 nm. To determine the purity of each sample, we performed an SDS-PAGE assay with Novex 10% Tricine gels (Invitrogen) and Coomassie Brilliant Blue staining enhanced with aluminum sulfate^{5,8}. The purities of final LinA2 and LinB solutions were > 95 % as determined by visual analysis (Figure S1). Activity assays were performed for each purification of LinA2 and LinB.

We prepared the staining solutions for SDS-Page gels according to Dyballa and Metzger⁵ but changed the staining protocol. The SDS-Page gels were shaken on a horizontal shaker in nanopure water for 10 minutes. After disposing of the water, we put the gel in the staining solution and let it shake overnight. After removing the staining solution, we washed the gel in nanopure water and then soaked it in destaining solution on a shaker for 2 hours. Activity

assays of the different purification steps of LinA2 and LinB were performed in tris-glycine buffer at pH 7.5 (200 mM glycine, 25 mM Trizma[®] base, final concentration). 25 μ M γ -HCH and LinA2 or 1 μ M β -HCH and LinB were incubated in a total reaction volume of 10 mL. For each time-point (0, 1, 2 and 4 minutes for reactions catalyzed by LinA2 and 0, 4, 8, and 16 min or 0, 5, 15, and 30 min for reactions catalyzed by LinB) a reactor was sacrificed by the addition of 4 mL ethyl acetate. All ethyl acetate extracts were analyzed with GC/MS. The purification procedure results in total protein yields of 6.3 mg LinA2 (from 1.7 g of frozen *E.coli* pellet) and 15.4 mg LinB (from 7.3 g of frozen *E.coli* pellet) with specific activities of 8.4 units/mg for LinA2 and 0.027 units/mg for LinB.

S3 Experimental setup and chemical analyses

An overview of experimental conditions in batch experiments, as well as analyte extraction for the kinetic and isotopic analyses of HCH transformation, and information for gas chromatography is shown in Table S1.

Temperature program for ZB-5MS column started at 70°C, followed by an isothermal hold of 2 min, then increased at 25°C/min to 120°C, at 5°C/min to 220°C and at 25°C/min to 280°C, finished by an isothermal hold of 2 min.⁶ The temperature programs for γ -DEXTM 120 and Rtx-1301 columns was 2 min at 70°C, 15°C/min to 110°C, 5°C/min to 200°C, 5°C/min to 220°C, and 25°C/min to 250°C (held for 2 min).¹⁷ For separation of compounds with the MEGA-DEX DAC-Beta column, the temperature program started with an isothermal hold at 70 °C for 2 min, followed by an increase of 5 °C/min to 180 °C, with an isothermal hold for 5 min, and finally an increase of 5 °C/min to 220 °C with an isothermal hold for 3 min. The temperature program for the Rxi 1 ms column began with an isothermal hold at 70 °C for 1 min, followed by an increase of 25 °C/min to 120 °C, to 200 °C at 5 °C/min, to 250 °C at 25 °C/min, and a final isothermal hold for 10 min.

S4 Data evaluation

S4.1 Conformational analysis

Data for calculating the predominant of two chair conformers of each HCH isomer is shown in Table S2. The free energy difference at standard conditions between the “regular”, that is thermodynamically more stable conformer and the flipped conformer (“flip”), $\Delta\Delta G^\circ$, was calculated with Marvin Beans (version 6.2, 2014, ChemAxon, <http://chemaxon.com>) The fraction of the more stable conformer, P, was obtained with this data and eqs. S1 to S3.

Table S1 Overview of experimental setup used for transformation experiments with different HCH isomers as well as gas chromatography columns used for concentration measurements and stable C and H isotope analysis.

Enzyme	HCH-isomer	Enzyme conc. (µg/mL)	Total activity ^a (units/L)	HCH conc. ^b (µM)	Acetone (vol-%)	Assay volume (mL)	solvent	GC-column	GC/IRMS
LinA2	(+)-α	0.7	4.4	35	1	150	n-hexane	γ-DEX TM 120 ^c	C: γ-DEX TM 120 ^c H: Rtx-1301 ^f
	(-)-α	0.01	0.03	35	1	150	n-hexane	γ-DEX TM 120 ^c	C: MEGA-DEX DAC Beta ^d H: Rtx-1301 ^f
	β	2.3 2.3	26.9 26.9	6 6	0.1 0.1	150 150	n-hexane n-hexane	ZB-5MS ^e ZB-5MS ^e	Rtx-1301 ^f Rtx-1301 ^f
	δ	2.1 2.1	17.7 17.7	35 35	0.7 0.7	150 150	n-hexane n-hexane	ZB-5MS ^e ZB-5MS ^e	Rtx-1301 ^f Rtx-1301 ^f
	α	13.9 14.5	0.8 0.4	35 25	1 1	150 150	n-hexane n-hexane	γ-DEX TM 120 ^c γ-DEX TM 120 ^c	C: MEGA-DEX DAC Beta ^d H: Rtx-1301 ^f C: MEGA-DEX DAC Beta ^d H: Rtx-1301 ^f
	β	2.6 13.1 8.2	0.09 0.5 0.2	0.8 6 25	0.02 1 1	450 800 175	n-hexane ethyl acetate n-hexane	ZB-5MS ^e ZB-5MS ^e ZB-5MS ^e	Rtx-1301 ^f Rtx-1301 ^f Rtx-1301 ^f
	δ	10.3	0.3	35	1	150	n-hexane	ZB-5MS ^e	Rxi 1 ms ^g
LinB									

^a calculated as the product of enzyme concentration and specific activity (section S2); ^b nominal concentrations;
^c 30 m length, 0.25 mm i.d., 25 µm film thickness, Supelco; ^d 25 m length, 0.25 mm i.d, 0.25 µm film thickness, MEGA;
^e 30 m length, 0.25 mm i.d., 25 µm film thickness, Phenomenex; ^f 30 m length, 0.32 mm i.d., 1 µm film thickness, Restek;
^g 60 m length, 0.32 mm i.d., 0.25 µm film thickness, Restek.

$$\Delta\Delta G^\circ = \Delta G_{\text{flip}}^\circ - \Delta G_{\text{regular}}^\circ = -RT \ln K \quad (\text{S1})$$

$$K = \frac{[\text{regular}]}{[\text{flip}]} \quad (\text{S2})$$

$$P = \frac{K \cdot 100}{K + 1} \quad (\text{S3})$$

where $\Delta\Delta G^\circ$ is the difference between the standard free energies of the two conformers, $\Delta G_{\text{flip}}^\circ$ and $\Delta G_{\text{regular}}^\circ$, respectively, R is the gas constant, T is the absolute temperature, and K is the equilibrium constant for the population of the two conformers.

To illustrate the time scales of changes of conformational mobility, we derived the frequency of conformational change, f_{flip} , and the corresponding lifetime of a conformer, τ_{conf} with eqs. S4 and S5 and the results are shown in Table S2.

$$f_{\text{flip}} = \frac{k_B T}{h} e^{(-\Delta G^\ddagger/RT)} \quad (\text{S4})$$

$$\tau_{\text{conf}} = \frac{1}{f_{\text{flip}}} \quad (\text{S5})$$

S4.2 Apparent kinetic isotope effects

General procedures of isotope analysis are listed in Pati et al.¹³. Non-linear regression for C and H isotope enrichment factors, ϵ_C and ϵ_H , and linear regression of $\delta^2\text{H}$ vs $\delta^{13}\text{C}$ for $\Lambda^{\text{H/C}}$ were carried out in Igor Pro (WaveMetrics). Fits were weighted with the standard deviation from triplicate isotope ratio measurements. All reported uncertainties represent 95% confidence intervals.

Apparent ^{13}C - and ^2H -kinetic isotope effects, ^{13}C - and ^2H -AKIEs, were obtained through two different procedures. First, all ^{13}C -AKIEs for HCH dehydrochlorination and hydrolytic dechlorination by LinA2 and LinB, respectively, were derived from ϵ_C with eq. S6 (eq. 5 of the main manuscript). The same procedure was used for calculating ^2H -AKIEs for hydrolytic dechlorination reactions of HCH isomers with LinB.

$$^{\text{h}}\text{E-AKIE} = \frac{1}{1 + n/x \cdot z \cdot \epsilon_E} \quad (\text{S6})$$

where E stands for C and H isotopes respectively, n is the number of atoms of element E, x stands for the number of such atoms at reactive positions, and z is the correction for intramolecular isotopic competition, and ϵ_E denotes the isotope enrichment factors. Parameter values for n , x , and z are given in Table S3. Second, ^2H -AKIEs for HCH dehydrochlorination by LinA2 follow from eq. S8 by evaluating eq. S7. This procedure is described in detail below in Section S4.2.3.

Table S2 $\Delta\Delta G^\circ$ of the two most stable conformers of α -, β -, and δ -HCH, fractional abundance of predominant conformer (P), activation energies for the respective conformational change, ΔG^\ddagger , and the lifetime of a conformer, τ_{conf} . All properties were calculated in Marvin Beans (version 6.2.0, 2014, ChemAxon, <http://chemaxon.com>). The blue bonds indicate the reactive H–C–C–Cl moieties for dehydrochlorination by LinA2 based on evidence from Schilling et al.¹⁷ and Trantirek et al.²¹.

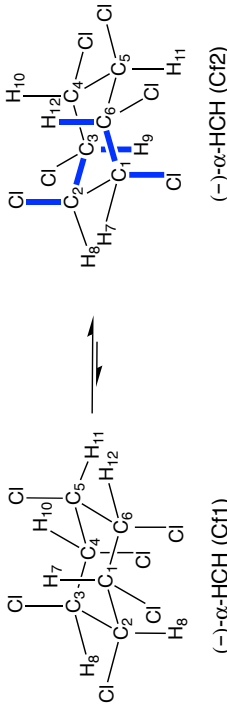
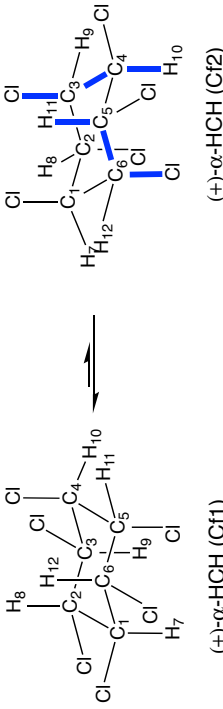
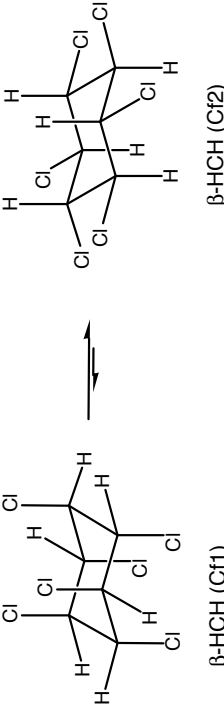
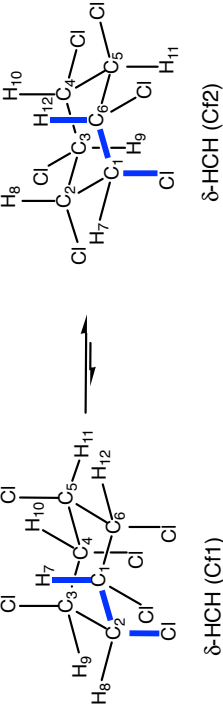
Isomer	$\Delta\Delta G^\circ$ (kJ/mol)	P (%)	ΔG^\ddagger (kJ/mol)	τ_{conf} (s)	Conformers
(–)- α -HCH	–10	98.2	44	$5 \cdot 10^{-6}$	 (–)- α -HCH (Cf1) (–)- α -HCH (Cf2)
(+)- α -HCH	–10	98.2	44	$5 \cdot 10^{-6}$	 (+)- α -HCH (Cf1) (+)- α -HCH (Cf2)
β -HCH	–22	100	45	$8 \cdot 10^{-6}$	 β-HCH (Cf1) β-HCH (Cf2)
δ -HCH	–15	99.8	57	$1 \cdot 10^{-3}$	 δ-HCH (Cf1) δ-HCH (Cf2)

Table S3 Parameter values n , x and z for calculation of apparent ^{13}C - and ^2H kinetic isotope effects associated with the dehydrochlorination and hydrolytic dechlorination of HCH isomers with eq. S6 (eq. 5 of the main manuscript).

Enzyme-substrate combination	¹³ C-AKIE			² H-AKIE		
	<i>n</i>	<i>x</i>	<i>z</i>	<i>n</i>	<i>x</i>	<i>z</i>
LinA2						
(-)-α-HCH	6	4	2	n.a. ^a		
(+)-α-HCH	6	4	2	n.a. ^a		
β-HCH	n.a. ^b			n.a. ^b		
γ-HCH	6	2	1	n.a. ^a		
δ-HCH	6	2	1	n.a. ^a		
LinB						
(-)-α-HCH	6	2	2	6	2	2
(+)-α-HCH	6	2	2	6	2	2
β-HCH	6	6	6	6	6	6
γ-HCH	n.a. ^c			n.a. ^c		
δ-HCH	6	1	1	6	1	1

^a AKIE approximiton not applicable due to large H isotope fractionation;

^b n.a. = not applicable due to the lack of reactivity with LinA2; ^c n.a. = not applicable due to the lack of reactivity with LinB.

S4.2.1 Dehydrochlorination by LinA2

(-)- α -HCH: The thermodynamically more stable conformer **Cf2** of (-)- α -HCH (Table S2) exhibits two trans-diaxial H-C-C-Cl moieties that are susceptible for dehydrochlorination by LinA2. Those moieties, H₁₂-C₆-C₁-Cl and H₉-C₂-C₃-Cl, are highlighted in blue in the molecular structures of the conformer in Table S2. Conformer **Cf1** does not contain any reactive sites.^{17,21} For data evaluation with eqs. S6 and S7, we assumed that (-)- α -HCH contains four reactive C atoms, namely C₁, C₆, C₂, and C₃ ($x = 4$), from which two are in intramolecular competition (C₆-C₁ and C₂-C₃, $z = 2$) because the dehydrochlorination is a concerted reaction (Table S3).

(+)- α -HCH: The thermodynamically less stable conformer **Cf2** of (+)- α -HCH conformers exhibits two trans-diaxial H-C-C-Cl moieties that are susceptible for dehydrochlorination by LinA2. Those moieties, H₁₂-C₅-C₆-Cl and H₁₀-C₄-C₃-Cl, are highlighted in blue the molecular structures of the conformer in Table S2. Conformer **Cf1** does not contain any reactive sites.^{17,21} n, x, z -values for (+)- α -HCH are identical to those of (-)- α -HCH.

β -HCH: β -HCH does not contain any reactive H-C-C-Cl moieties for dehydrochlorination by LinA2.

γ -HCH: The reactive moieties of γ -HCH for dehydrochlorination by LinA2 have been discussed in detail in Schilling et al.¹⁷ and the results are shown in Table S3.

δ -HCH: The two most stable δ -HCH conformers (Table S2) both exhibit one trans-diaxial H-C-C-Cl moiety that is susceptible for dehydrochlorination by LinA2. Those moieties, H₁₂-C₆-C₁-Cl in the more stable conformer **Cf2** and H₇-C₁-C₂-Cl in **Cf1**, are highlighted in blue in the molecular structures of the conformers in Table S2. For data evaluation with eqs. S6 and S7, we assumed that each δ -HCH conformer contains two reactive C atoms ($x = 2$) which are not in intramolecular competition ($z = 1$) (table S2: $x=4$, $z=2$) because the dehydrochlorination is a concerted reaction.

S4.2.2 Hydrolytic dechlorination by LinB

(-)- α -HCH and (+)- α -HCH: Even though a preference for hydrolytic dechlorination for equatorial chlorine atoms has been postulated,⁹ assigning reactive positions from molecular structure is less straightforward. Our assignment of reactive positions is based on the exclusive observation of two pentachlorocyclohexanol isomers as hydrolysis products of (-)- α -HCH.¹⁵ The number of C and H atoms at reactive sites in intramolecular competition was thus set to $x = z = 2$.

β -HCH: All C and H atoms of **Cf2** of β -HCH are considered equally reactive.¹⁴ The number of C and H atoms at reactive sites in intramolecular competition was thus set to $x = z = 6$.

γ -HCH: γ -HCH does not react with LinB.

δ -HCH: Hydrolysis of δ -HCH is highly regioselective¹⁴ and only the equatorial C-Cl opposite the axial C-Cl is transformed. The number of C and H atoms at reactive sites in intramolecular competition was thus set to $x = z = 1$.

S4.2.3 Calculation of ^2H -AKIE values associated with HCH dehydrochlorination by LinA2

We derived the ^2H -AKIEs for the dehydrochlorination of HCH isomers by LinA2 following procedures described in Schilling et al.¹⁷ for γ -HCH and are they summarized here for each substrate-enzyme combination. We quantified the observable H isotope fractionation in an isotopomer-specific kinetic model, eq.S7, by fitting the ^2H -AKIEs with eq. S8 using Aquasim.¹⁶

$$\frac{dc_i^E}{dt} = \sum_j \nu_i \cdot \omega_i^E \cdot k_j^E \cdot c_i^E \quad (\text{S7})$$

$$^h\text{E-AKIE} = \frac{k_h^E}{k_l^E} \quad (\text{S8})$$

where j designates the reaction of light and heavy isotopologues, c_i^E is the concentration of a HCH isotopomer i of element E, ν_i is the stoichiometric coefficient indicating decay or formation of an isotopomer, ω_i^E is the probability of isotopomer i to have a heavy or light isotope at the reactive position, and k_j^E is the first order rate constant for reaction of an isotopomer according to the presence of the light (l) or heavy (h) isotope at the reactive position (k_l^E and k_h^E). Note that the validity of this approach was tested by applying eq. S7 to data for C isotope fractionation and comparing the calculated ^{13}C -AKIE from eq. S8 with that of obtained with eq. S6. As shown previously,¹⁷ both procedures resulted in identical ^{13}C -AKIEs.

Table S4 lists the isotopomers, i , considered in the modeling exercise for δ -HCH, (+)- α -HCH, and (–)- α -HCH, and designates the position of heavy C and H substitution. The parameter quantifying the probability of isotopomer i to exhibit a heavy or light C or H isotope at the reactive position, ω^E takes the conformational mobility and the ensuing change in reactive position into account.

Table S4 Carbon and hydrogen isotopomers considered in the isotopomer-specific analysis of C and H isotope fractionation associated with the dehydrochlorination and hydrolytic dechlorination of HCH isomers by LinA2 and LinB, respectively. Data for P as well as the C and H atom numbers refer to molecule structures drawn in Table S2.

Carbon isotopes												
Isotopomer	Position of isotopic substitution						δ -HCH/LinA2		$(+)\text{-}\alpha$ -HCH/LinA2		δ -HCH/LinB	
	C ₁	C ₂	C ₃	C ₄	C ₅	C ₆	$\omega^{12\text{C}}$	$\omega^{13\text{C}}$	$\omega^{12\text{C}}$	$\omega^{13\text{C}}$	$\omega^{12\text{C}}$	$\omega^{13\text{C}}$
HCH1	¹² C	¹² C	¹² C	¹² C	¹² C	¹² C	1	0	1	0	1	0
HCHh1	¹³ C	¹² C	¹² C	¹² C	¹² C	¹² C	0	1	1	0	1	0
HCHh2	¹² C	¹³ C	¹² C	¹² C	¹² C	¹² C	P	1-P	1	0	1	0
HCHh3	¹² C	¹² C	¹³ C	¹² C	¹² C	¹² C	1	0	0.5	0.5	1	0
HCHh4	¹² C	¹² C	¹² C	¹³ C	¹² C	¹² C	1	0	0.5	0.5	0	1
HCHh5	¹² C	¹² C	¹² C	¹² C	¹³ C	¹² C	1	0	0.5	0.5	1	0
HCHh6	¹² C	¹² C	¹² C	¹² C	¹² C	¹³ C	1-P	P	0.5	0.5	1	0
Hydrogen isotopes												
isotopomer	Position of isotopic substitution						δ -HCH/LinA2		$(+)\text{-}\alpha$ -HCH/LinA2		δ -HCH/LinB	
	H ₇	H ₈	H ₉	H ₁₀	H ₁₁	H ₁₂	$\omega^{1\text{H}}$	$\omega^{2\text{H}}$	$\omega^{1\text{H}}$	$\omega^{2\text{H}}$	$\omega^{1\text{H}}$	$\omega^{2\text{H}}$
HCH1	¹ H	¹ H	¹ H	¹ H	¹ H	¹ H	1	0	1	0	1	0
HCHh7	² H	¹ H	¹ H	¹ H	¹ H	¹ H	P	1-P	1	0	1	0
HCHh8	¹ H	² H	¹ H	¹ H	¹ H	¹ H	1	0	1	0	1	0
HCHh9	¹ H	¹ H	² H	¹ H	¹ H	¹ H	1	0	1	0	1	0
HCHh10	¹ H	¹ H	¹ H	² H	¹ H	¹ H	1	0	0.5	0.5	0	1
HCHh11	¹ H	¹ H	¹ H	¹ H	² H	¹ H	1	0	0.5	0.5	1	0
HCHh12	¹ H	¹ H	¹ H	¹ H	¹ H	² H	1-P	P	1	0	1	0

S4.3 Interpretation of H isotope fractionation associated with α -HCH transformation by LinA2 and LinB

The chromatographic separation of α -HCH enantiomers peaks for $^2\text{H}/^1\text{H}$ measurements was insufficient due to peak broadening in the high temperature conversion Cr reactor of the GC/IRMS conversion interface. In the absence of enantiomer-specific $\delta^2\text{H}$ data, the interpretation of H isotope fractionation of $(-)\text{-}\alpha$ - and $(+)\text{-}\alpha$ -HCH during dehydrochlorination as well as $(-)\text{-}\alpha$ -HCH during hydrolytic dechlorination by LinB was made based on assumptions derived from model calculations illustrated in the following. All model calculations were carried out in Matlab based on a simple mathematical model for first order disappearance of ^2H and ^1H isotopologues of $(-)\text{-}\alpha$ - and $(+)\text{-}\alpha$ -HCH. The model code is shown below in Section S4.3.3.

S4.3.1 α -HCH dehydrochlorination by LinA2

Low enzyme concentration. Experiments with a racemic α -HCH at low LinA2 concentrations ($0.01\ \mu\text{g}/\text{mL}$) revealed H isotope fractionation as shown in Figure 1F. We hypothesize that this H isotope fractionation originates from $(+)\text{-}\alpha$ -HCH because of (a) the small extent of transformation of $(+)\text{-}\alpha$ -HCH is associated with a large ^2H -AKIE ($^2\text{H}\text{-AKIE}_{(+)\text{-}\alpha\text{-HCH}} = 6.7$). Note that a C isotope fractionation of $(+)\text{-}\alpha$ -HCH would be too small to be detected at such small turnover. (b) The lack of observed C isotope fractionation for $(-)\text{-}\alpha$ -HCH (Figure 1E) implying that H isotope fractionation should also be absent for this α -HCH enantiomer ($^2\text{H}\text{-AKIE}_{(-)\text{-}\alpha\text{-HCH}} = 1$).

Figure S2A shows the calculated changes of $(-)\text{-}\alpha$ - and $(+)\text{-}\alpha$ -HCH concentrations based on the observation that the $(-)\text{-}\alpha$ -enantiomer reacts approximately 20 times faster than the $(+)\text{-}\alpha$ -enantiomer over the reactive period of 10 min (Table S6, Figures 1d and S2A). Panels S2B and C illustrate the observable H isotope fractionation for the $(-)\text{-}\alpha$ - and $(+)\text{-}\alpha$ -enantiomers as well as for the combined, bulk α -HCH. All calculations assumed identical initial $\delta^2\text{H}$ -values of $(-)\text{-}\alpha$ - and $(+)\text{-}\alpha$ -HCH of $\delta^2\text{H}_0 = -100\text{‰}$. Panel S2C reveals that H isotope fractionation of bulk α -HCH can be observed from the combination of large H isotope fractionation for $(+)\text{-}\alpha$ -HCH while no H isotope fractionation occurs in $(-)\text{-}\alpha$ -HCH. Panels S2D to F illustrate that identical H isotope fractionation behavior can be observed if $(-)\text{-}\alpha$ - and $(+)\text{-}\alpha$ -HCH exhibit different initial $\delta^2\text{H}$ -values. For this illustration, they were arbitrarily set to $\delta^2\text{H}_{(-)\alpha_0} = -130\text{‰}$ and $\delta^2\text{H}_{(+)\alpha_0} = -70\text{‰}$.

High enzyme concentration. In experiments at higher LinA2 concentration ($0.7\ \mu\text{g}/\text{mL}$), we assigned the observable H isotope fractionation to $(+)\text{-}\alpha$ -HCH given that (a) $(-)\text{-}\alpha$ -HCH was quickly transformed to a residual concentration of approximately $3\ \mu\text{M}$ (Figure 1G) and (b) the dehydrochlorination of $(-)\text{-}\alpha$ -enantiomer did not reveal any C isotope fractionation (see above). To that end, we derived $\delta^2\text{H}$ values for $(+)\text{-}\alpha$ -HCH from an isotopic mass balance approach in eqs.S9 and S10 assuming identical initial $\delta^2\text{H}$ -values of $(-)\text{-}\alpha$ - and $(+)\text{-}\alpha$ -HCH of $\delta^2\text{H}_0 = -100\text{‰}$. Note that this procedure was validated by applying it to data for C isotope fractionation where the two α -HCH were baseline-separated during analysis by GC/IRMS.

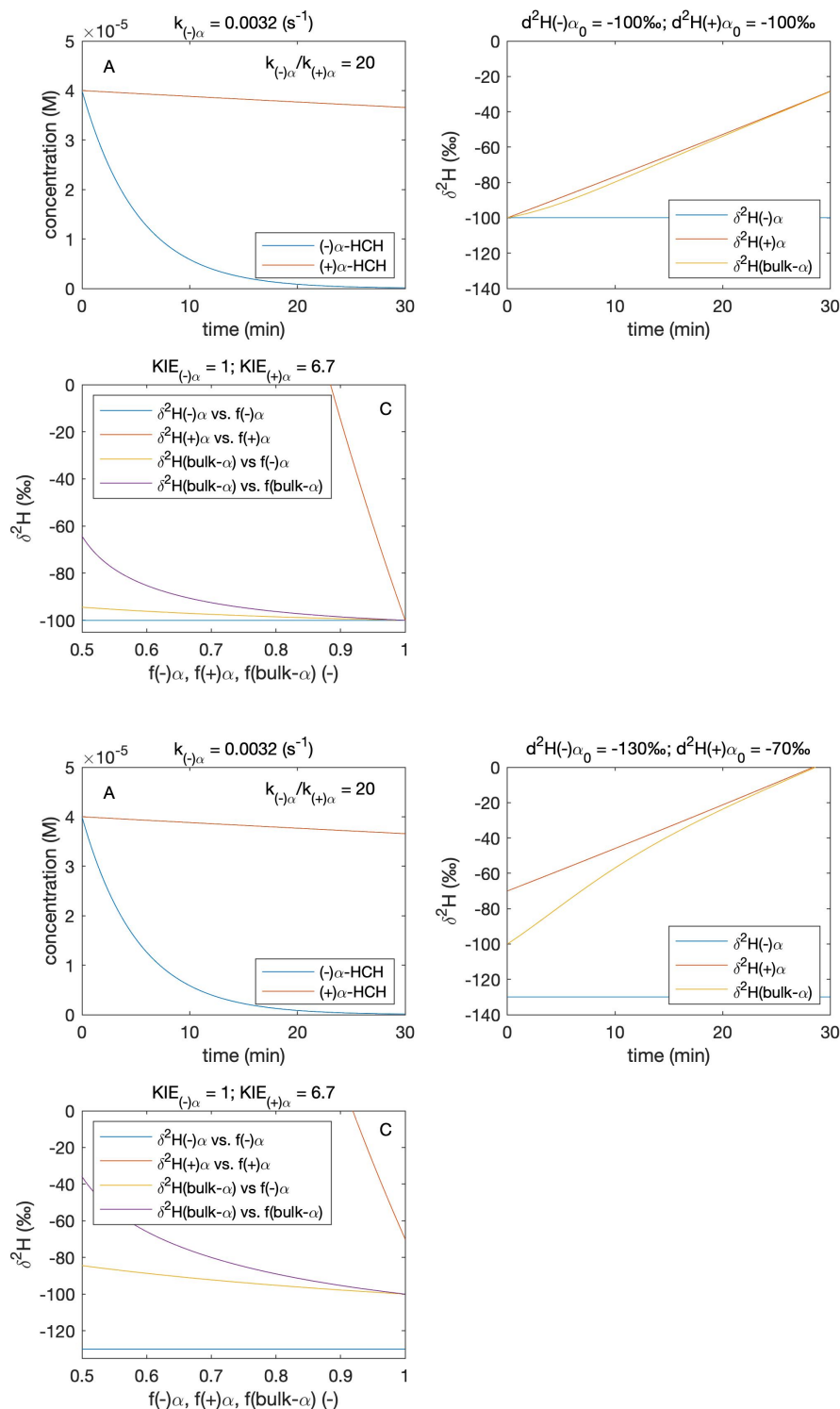


Figure S2 Simulation of H isotope fractionation mimicking experiments with α -HCH and small concentrations of LinA2 ($0.01 \mu\text{g/mL}$). Panels A and D show the concentration changes of the two α -HCH enantiomers. Panels B and E illustrate changes of $\delta^2\text{H}$ of $(-)\alpha\text{-HCH}$, $(+)\alpha\text{-HCH}$, and bulk- $\alpha\text{-HCH}$ vs. time. Panels C and F display the same data vs. fraction, f , of remaining reactant. Calculations shown in panels A-C are for identical initial $\delta^2\text{H}$ values of -100‰ . Calculations shown in panels D-F were made with $\delta^2\text{H}_0$ of -130‰ and -70‰ for $(-)\alpha\text{-HCH}$ and $(+)\alpha\text{-HCH}$, respectively.

Hydrogen isotope enrichment factors for (+)- α -HCH were then derived following standard procedures (i.e., eq. 3).

$$\delta^2\text{H}_{\text{measured}}^0 = \delta^2\text{H}_{(-)\text{-}\alpha\text{-HCH}}^0 = \delta^2\text{H}_{(+)\text{-}\alpha\text{-HCH}}^0 \quad (\text{S9})$$

$$\delta^2\text{H}_{(+)\text{-}\alpha\text{-HCH}} = \left(\delta^2\text{H}_{\text{measured}} - \delta^2\text{H}_{(-)\text{-}\alpha\text{-HCH}} \cdot \frac{[(-)\text{-}\alpha\text{-HCH}]}{[\alpha\text{-HCH}]} \right) \cdot \frac{[\alpha\text{-HCH}]}{[(+)\text{-}\alpha\text{-HCH}]} \quad (\text{S10})$$

where $\delta^2\text{H}_{\text{measured}}$ are H isotope signatures measured for bulk- α -HCH, that is both α -enantiomers, $[(+)\text{-}\alpha\text{-HCH}]$ and $[(-)\text{-}\alpha\text{-HCH}]$ are the concentrations of (+)- α -HCH and (–)- α -HCH, respectively, and $[\alpha\text{-HCH}]$ is the concentration of bulk- α -HCH.

S4.3.2 Hydrolytic dechlorination of α -HCH by LinB

The H isotope fractionation shown in Figure 2F of the main manuscript would correspond to an ϵ_{H} of $-43 \pm 9\text{‰}$ if assigned to the transformation of (–)- α -HCH. Note that (+)- α -HCH does not react over the time scale of our experiment. This ϵ_{H} -value is, however, too negative to be consistent with the observed masking of C isotope fractionation ($\epsilon_{\text{C}} = -3.0 \pm 1.4\text{‰}$) for the hydrolytic dechlorination of (–)- α -HCH. In the absence of masking, the ϵ_{C} -value should be in the range of -11‰ as observed for δ -HCH. We hypothesize that the H isotope fractionation of (–)- α -HCH was also masked and that the H isotope fractionation of bulk α -HCH shown in Figure 2F was at least in part, an artifact of different initial $\delta^2\text{H}$ -values ($\delta^2\text{H}_0$) of the two α -HCH enantiomers in the racemic mixture

To confirm our hypothesis, we quantified the concentration changes and H isotope fractionation of α -HCH enantiomers with a 10-fold difference in reaction rate constants observed at initial stages of the reaction (500 min, Figures 2d and S3A, Table S6), a ^2H -AKIE of unity (1), as well as different initial $\delta^2\text{H}$ -values ($\delta^2\text{H}(-)\alpha_0 = -100\text{‰}$ and $\delta^2\text{H}(+)\alpha_0 = -40\text{‰}$, $\delta^2\text{H}(\text{bulk-}\alpha)_0 = -70\text{‰}$). Note that experiments with LinB were carried out with a different batch of α -HCH than experiments with LinA2. Figure panels S3B and C show that during the transformation of (–)- α -HCH, the measured $\delta^2\text{H}$ of the bulk- α -HCH is increasingly determined by the less reactive (+)- α enantiomer. Any H isotope fractionation could thus have been caused by the preferential reaction of the isotopically light (–)- α -enantiomer (more negative $\delta^2\text{H}$) and concomitant accumulation of isotopically heavy (+)- α -enantiomer even with a ^2H -AKIE of 1. This phenomenon (i) confirms that the observed H isotope fractionation could have been masked in analogy to the masking of C isotope fractionation and (ii) precludes the quantification of ϵ_{H} -values that can be assigned to a reaction of α -HCH.

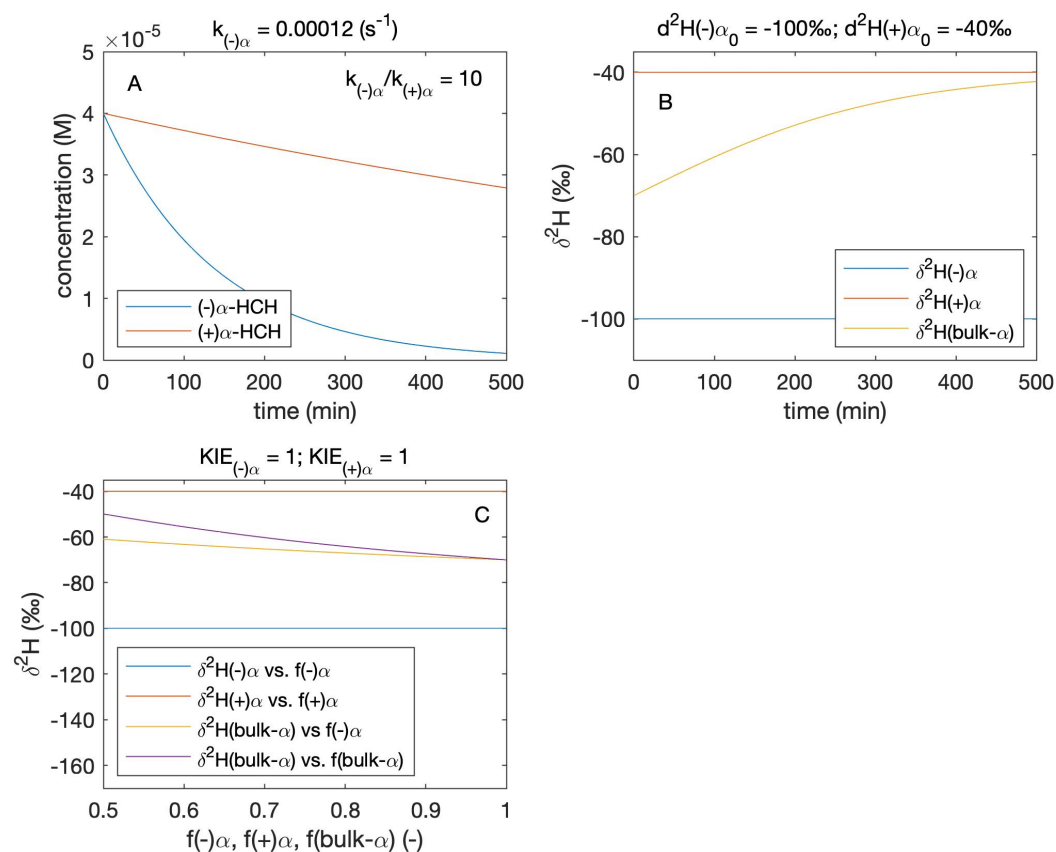


Figure S3 Simulation of H isotope fractionation mimicking experiments with α -HCH and LinB. Panel A shows the concentration changes of the two α -HCH enantiomers. Panel B illustrates changes of $\delta^2\text{H}$ of $(-)\alpha$ -HCH, $(+)\alpha$ -HCH, and bulk- α -HCH vs. time. Panel C displays the same data vs. fraction, f , of remaining reactant. All calculations were made with $\delta^2\text{H}_0$ of -100‰ and -40‰ for $(-)\alpha$ - and $(+)\alpha$ -HCH, respectively.

S4.3.3 Matlab Scripts

```
1 function dcdt = reactorodela(t,c)
2 %% reactions
3 % A -> reaction of (-)alpha-HCH enantiomer
4 % B -> reaction of (+)alpha-HCH enantiomer
5
6 %% species
7 % 1 (-)alpha-HCH light isotopologue
8 % 2 (-)alpha-HCH heavy isotopologue
9 % 3 (+)alpha-HCH light isotopologue
10 % 4 (+)alpha-HCH heavy isotopologue
11
12 %% variables
13 global kaL kaH kbL kbH
14 global KIEa KIEb
15
16 %% expressions
17 kaH = kaL/KIEa;
18 kbH = kbL/KIEb;
19
20 %% others
21 dcdt=zeros(size(c));
22
23 %% equation
24 dcdt(1) = -kaL*c(1);
25 dcdt(2) = -kaH*c(2);
26 dcdt(3) = -kbL*c(3);
27 dcdt(4) = -kbH*c(4);
```

```
1 %% isoscript model alpha-HCH
2 clear all
3 close all
4 clc
5 %% variables
6 global kaL kbL %kaH kbH
7 global KIEa KIEb
8
9 %% data input
10 kaL = 5e-5; % s-1
11 kbL = kaL/500; % s-1
12 KIEa = 1.000; % -
13 KIEb = 1.000; % -
14 Rstd = 0.01122; % -
15
16 %% initial conditions
17 Atot0 = 4e-5; % M
```

```

18 Btot0 = 4e-5;    % M
19 dhEA0 = -100;    %
20 dhEB0 = -40;
21
22 %% derived parameters
23 RA0 = (dhEA0/1000+1)*Rstd;
24 RB0 = (dhEB0/1000+1)*Rstd;
25 RAB0 = ((dhEA0+dhEB0)/2/1000+1)*Rstd;
26
27 AL0 = Atot0 / (1 + RA0);
28 AH0 = AL0 * RA0;
29 BL0 = Btot0 / (1 + RB0);
30 BH0 = BL0 * RB0;
31 c0 = [AL0 AH0 BL0 BH0];
32
33 %% define calculation
34 max_time = 30*86400;
35 tspan = [0 max_time];
36
37 %% solve differential equations
38 options = odeset('reltol',1e-10,'abstol',1e-15);
39 [t,c] = ode15s(@reactorodelb,tspan,c0,options);
40
41 %% evaluating results: concentration, time
42 AL = c(:,1);
43 AH = c(:,2);
44 BL = c(:,3);
45 BH = c(:,4);
46 time = t/3600;
47
48 %% evaluating results: isotope ratios and signatures
49 A = AL + AH;
50 B = BL + BH;
51 RA = c(:,2)./c(:,1);
52 RB = c(:,4)./c(:,3);
53 dhEA = (RA/Rstd - 1) * 1000;
54 dhEB = (RB/Rstd - 1) * 1000;
55 fA = (c(:,2)+c(:,1))/(c(1,1)+c(1,2));
56 fB = (c(:,4)+c(:,3))/(c(1,3)+c(1,4));
57 lnRA = log(RA/RA0);
58 lnfA = log(fA);
59 lnRB = log(RB/RB0);
60 lnfB = log(fB);
61
62 %% Calculation (observable) bulk parameters
63 ABL = (c(:,1)+c(:,3));
64 ABH = (c(:,2)+c(:,4));
65
66 RAB = ABH./ABL;
67 dhEAB = (RAB/Rstd - 1) * 1000;

```

```

68 fAB = (c(:,1)+c(:,2)+c(:,3)+c(:,4))/(c(1,1)+c(1,2)+c(1,3)+c(1,4));
69 lnRAB = log(RAB/RAB0);
70 lnfAB = log(fAB);
71
72 %% plotting results
73
74 figure
75 title221 = ['k_{(-)\alpha} = 5^{.10^{-5}} (s^{-1})'];
76 title222 = ['d^2H(-)\alpha_0 = ', num2str(dhEA0,3), ' ; d^2H(+)\alpha_0 = ',
77 num2str(dhEB0,3), ' '];
78 title223 = ['KIE_{(-)\alpha} = ', num2str(KIEa,5), ' ; KIE_{(+)\alpha} = ',
79 num2str(KIEb,5)];
80 title224 = 'Semilog plot';
81 fontsi = 10;
82
83 subplot(2,2,1)
84 plot(time*60, A, time*60, B)
85 ylim([0 5e-5]);
86 xlim([0 500]);
87 xlabel('time (min)');
88 ylabel('concentration (M)');
89 title(title221,'FontSize', fontsi, 'FontWeight', 'normal');
90 legend('(-)\alpha-HCH', '(+)\alpha-HCH', 'Location', 'southwest');
91 text(20, 4.5e-5, 'k_{(-)\alpha}/k_{(+)\alpha} = 500')
92
93 subplot(2,2,2)
94 plot(time*60, dhEA, time*60, dhEB, time*60, dhEAB)
95 ylim([-110 -35]);
96 xlim([0 500]);
97 xlabel('time (min)');
98 ylabel('\Delta^2H ( )');
99 title(title222,'FontSize', fontsi, 'FontWeight', 'normal');
100 legend('\Delta^2H(-)\alpha', '\Delta^2H(+)\alpha', '\Delta^2H(bulk-\alpha)',
101 'Location', 'southeast');
102
103 subplot(2,2,3);
104 plot(fA, dhEA, fB, dhEB, fA, dhEAB, fAB, dhEAB)
105 xlim([0.5 1]);
106 ylim([-170 -35]);
107 xlabel('f(-)\alpha, f(+)\alpha, f(bulk-\alpha) (-)');
108 ylabel('\Delta^2H ( )');
109 title(title223,'FontSize', fontsi, 'FontWeight', 'normal');
110 legend('\Delta^2H(-)\alpha vs. f(-)\alpha', '\Delta^2H(+)\alpha vs. f(+)\alpha',
111 '\Delta^2H(bulk-\alpha) vs f(-)\alpha', '\Delta^2H(bulk-\alpha) vs.
112 f(bulk-\alpha)', 'Location', 'southwest');
113
114 print -djpeg -r300 1b

```

S5 Additional Data

S5.1 Chemical structures of substrates and products

Figure S4 shows the chemical structures of all HCH isomers used as substrates in the present and predecessor study,¹⁷ as well as the those of identified product isomers. Figure S5 lists all possible stereoisomers of PCCH.

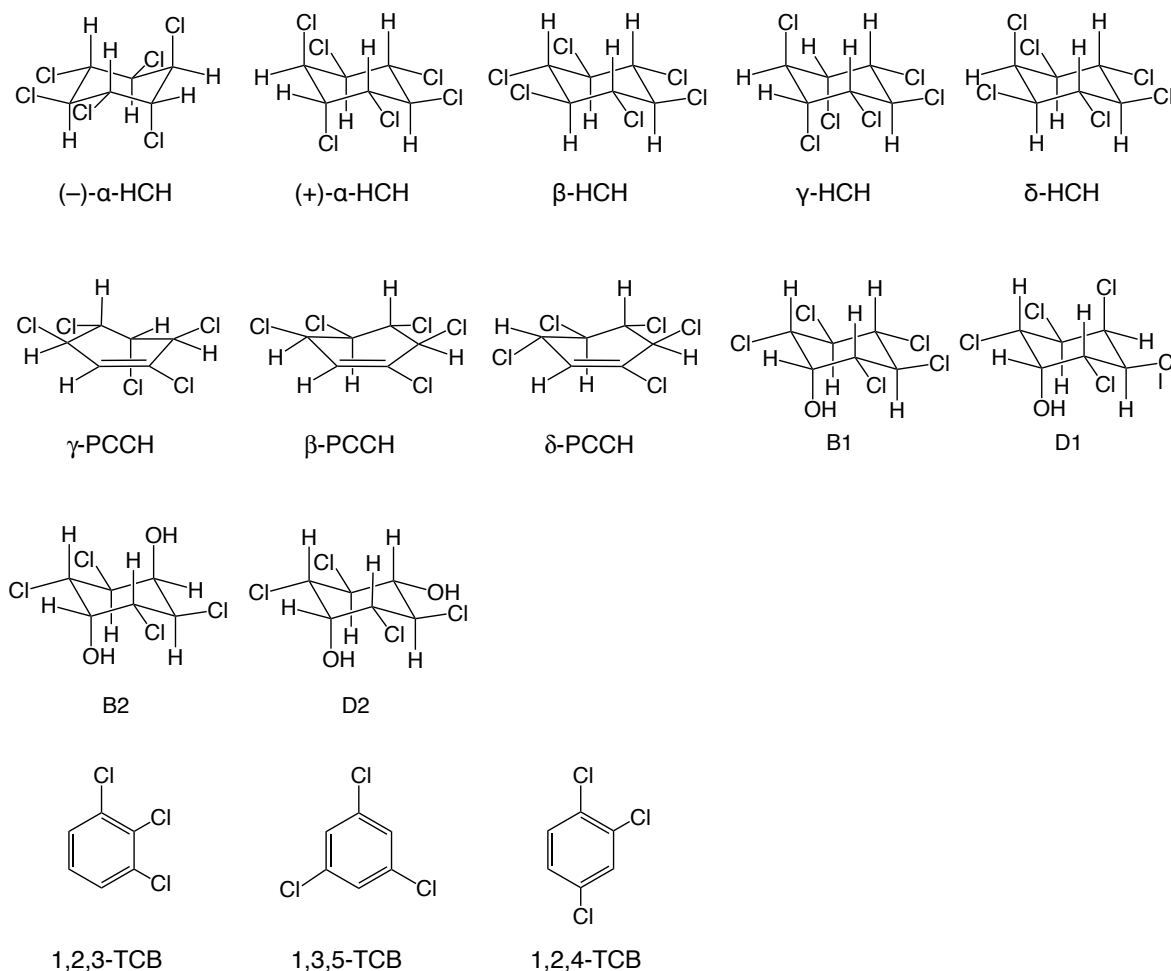


Figure S4 Overview over the chemical structures of substrates and products. All structures are shown in their most stable conformer. For the PCCHs only one enantiomer is shown. Abbreviations used: HCH for hexachlorocyclohexane isomers; PCCH for pentachlorocyclohexene isomers; B1, D1 for pentachlorocyclohexanol isomers; B2, D2 for tetrachlorocyclohexanediol isomers; TCB for trichlorobenzene isomers.

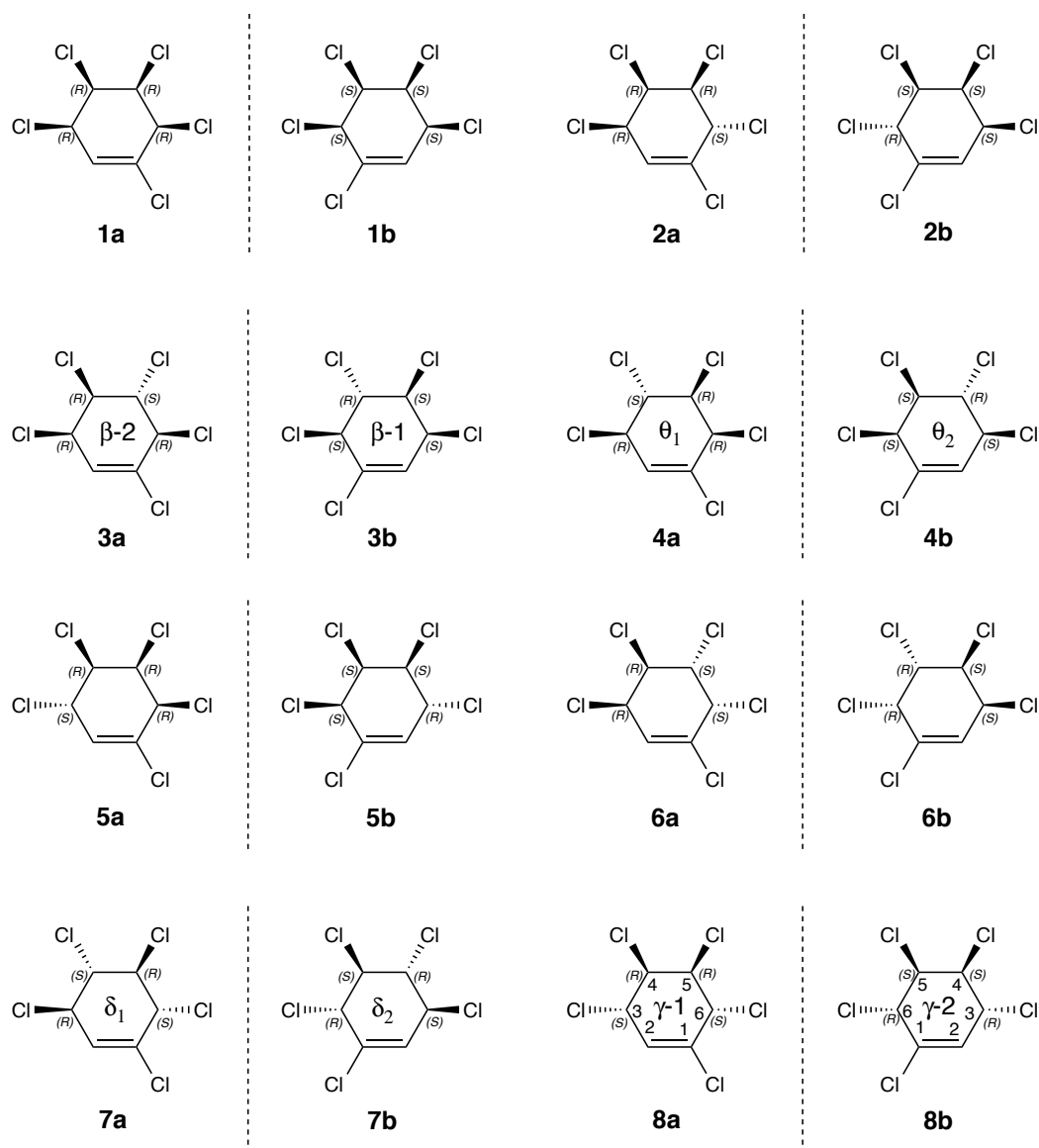


Figure S5 Configurations of all sixteen possible pentachlorocyclohexene (PCCH) stereoisomers. Dashed lines indicate mirror planes. Greek letters indicate the PCCH enantiomers that are relevant for this study, whereby for enantiomers with subscripts the absolute configurations are unknown (δ -PCCH and θ -PCCH). For β -PCCH and γ -PCCH the absolute configurations of the enantiomers are known and the numbering indicates the elution order on a β -cyclodextrin fused silica capillary column.^{12,19–21} For compounds **8a** and **8b** (γ -PCCH1 and γ -PCCH2, respectively) the numbering for the carbon atoms in the ring is given, so it can be seen that γ -PCCH1 and γ -PCCH2 correspond to 1, 3*S*, 4*R*, 5*R*, 6*S*-PCCH and 1, 3*R*, 4*S*, 5*S*, 6*R*-PCCH, respectively. The numbering for γ -PCCH is exemplary and is analogous for all sixteen stereoisomers shown. Compound **3a** (β -PCCH2) and **3b** (β -PCCH1) are the products of enantioselective dehydrochlorinations of (–)- α -HCH and (+)- α -HCH, respectively, catalyzed by LinA2 or by LinA1 (^{19,20}, this work). When acting on γ -HCH, LinA2 enantioselectively produces compound **8b**, whereas LinA-type2 (closely related to LinA1) produces a racemic mixture of compounds **8a** and **8b**.^{19,21} It needs to be noted that in Suar et al.²⁰ and Shrivastava et al.¹⁹, the absolute configurations of the β -PCCH enantiomers have been mistaken for those of the θ -PCCH enantiomers.

S5.2 Survey of investigations of aerobic HCH biodegradation and -transformation with compound-specific isotope analysis

Table S5 Survey of state-of-the art on stable-isotope-based investigations of aerobic HCH biotransformation as well as studies in abiotic model systems and theoretical work that targets the same reactions, namely hydrolytic dechlorination and dehydrochlorination (see Scheme 2 in main manuscript). Letters “C”, “H”, and “Cl” stand for the isotopic element investigated in each study.

System	Elements	(+)- α -HCH	(-)- α -HCH	β -HCH	γ -HCH	δ -HCH
Whole organisms						
<i>S. indicum</i> B90A	C	Bashir et al. ²	Bashir et al. ²		Bashir et al. ²	
<i>S. japonicum</i> UT26	C	Bashir et al. ²	Bashir et al. ²		Bashir et al. ²	
Purified enzymes						
LinA1	C, H				Schilling et al. ¹⁷	
LinA2	C, H	this study	this study	this study ^a	Schilling et al. ¹⁷	this study
LinB	C, H	this study	this study	this study	this study ^a	this study
Abiotic model systems						
Alkaline solution	C	(Zhang et al. ²²) ^b				
Computations						
LinA	C, H, Cl		Manna et al. ¹¹	Manna et al. ¹¹	Manna et al. ¹¹	Manna et al. ¹¹
Field studies						
Unspecified field site	C	(Bashir et al. ³) ^b				
Bitterfeld-Wolfen, Germany	C	Liu et al. ¹⁰	Liu et al. ¹⁰	Bashir et al. ³	Bashir et al. ³	Bashir et al. ³
Pesticide facility, FL, USA	C	(Chartrand et al. ⁴) ^b		Chartrand et al. ⁴	Liu et al. ¹⁰	Liu et al. ¹⁰
				Chartrand et al. ⁴	Chartrand et al. ⁴	Chartrand et al. ⁴

^a no reactivity of this enzyme-substrate combination as discussed in the present study; ^b α -HCH enantiomers not specified.

S5.3 Reaction rate constants and catalytic efficiencies

We used the Levenberg-Marquardt algorithm in Copasi⁷ to solve first-order ordinary differential equations with which we determined the first order rate constant, k_{obs} , for the disappearance of the substrate and the appearance of intermediates and products (Table S6). The reported differences among k_{obs} -values and catalytic efficiencies, $k_{\text{cat}}/K_{\text{m}}$, for each substrate-enzyme combination, are due to the inherent variability among biological replicates as well as differences of substrate concentrations.

Table S6 Reaction rate constants, k_{obs} , and catalytic efficiencies, $k_{\text{cat}}/K_{\text{m}}$, from individual experiments with different HCH isomers with LinA2 and LinB, respectively. We did not observe any transformation of β -HCH by LinA2 and no transformations of (+)- α -HCH and γ -HCH by LinB.

Substrate	Reaction	k_{obs} (s ⁻¹)	$k_{\text{cat}}/K_{\text{m}}$ (M ⁻¹ s ⁻¹)
LinA2			
(-)- α -HCH ^a	(-)- α -HCH \rightarrow β -PCCH	$(3.2 \pm 0.2) \cdot 10^{-3}$	$(5.6 \pm 0.1) \cdot 10^6$
(-)- α -HCH ^b	(-)- α -HCH \rightarrow β -PCCH	$(1.6 \pm 0.2) \cdot 10^{-3}$	$(4.3 \pm 0.1) \cdot 10^4$
	β -PCCH \rightarrow TCB	$(1.6 \pm 0.1) \cdot 10^{-4}$	$(4.3 \pm 0.1) \cdot 10^3$
(+)- α -HCH ^b	(+)- α -HCH \rightarrow β -PCCH	$(3.4 \pm 0.2) \cdot 10^{-5}$	$(8.9 \pm 0.1) \cdot 10^2$
	β -PCCH \rightarrow TCB	$(3.2 \pm 0.2) \cdot 10^{-4}$	$(8.6 \pm 0.1) \cdot 10^3$
β -HCH	—	—	—
γ -HCH	γ -HCH \rightarrow γ -PCCH	$(9.1 \pm 0.2) \cdot 10^{-4}$	$(1.7 \pm 0.1) \cdot 10^4$
	γ -PCCH \rightarrow 1,2,4-TCB	$(1.6 \pm 0.1) \cdot 10^{-3}$	$(2.9 \pm 0.1) \cdot 10^4$
δ -HCH	δ -HCH \rightarrow δ -PCCH	$(1.1 \pm 0.1) \cdot 10^{-4}$	$(9.0 \pm 0.1) \cdot 10^2$
	δ -PCCH \rightarrow 1,2,3-TCB	$(1.1 \pm 0.1) \cdot 10^{-6}$	$(8.9 \pm 0.7) \cdot 10^1$
	δ -PCCH \rightarrow 1,2,4-TCB	$(1.5 \pm 0.1) \cdot 10^{-5}$	$(1.3 \pm 0.1) \cdot 10^2$
LinB			
(-)- α -HCH	(-)- α -HCH \rightarrow PCHL	$(1.2 \pm 0.1) \cdot 10^{-4}$	$(2.8 \pm 0.1) \cdot 10^2$
(+)- α -HCH	—	—	—
β -HCH ^c	β -HCH \rightarrow B1	$(1.2 \pm 0.1) \cdot 10^{-3}$	$(3.5 \pm 0.1) \cdot 10^4$
β -HCH ^d	β -HCH \rightarrow B1	$(3.7 \pm 0.2) \cdot 10^{-4}$	$(9.4 \pm 0.1) \cdot 10^2$
γ -HCH	—	—	—
δ -HCH	δ -HCH \rightarrow D1	$(3.7 \pm 0.2) \cdot 10^{-4}$	$(1.2 \pm 0.1) \cdot 10^3$

^a 0.01 $\mu\text{g/mL}$ LinA2 ^b 0.7 $\mu\text{g/mL}$ LinA2 ^c 0.8 μM initial β -HCH concentration

^d 6 μM initial β -HCH concentration

S5.4 Pentachlorocyclohexenes from α -HCH

From each α -HCH enantiomer, different pentachlorocyclohexenes (PCCHs) can theoretically be formed in trans-diaxial elimination reactions. The possible reaction pathways from the less stable conformer of each enantiomer (Table S2) are also shown. Each conformer has two reactive sites. From each site the same PCCH will be formed in a trans-diaxial elimination reaction.

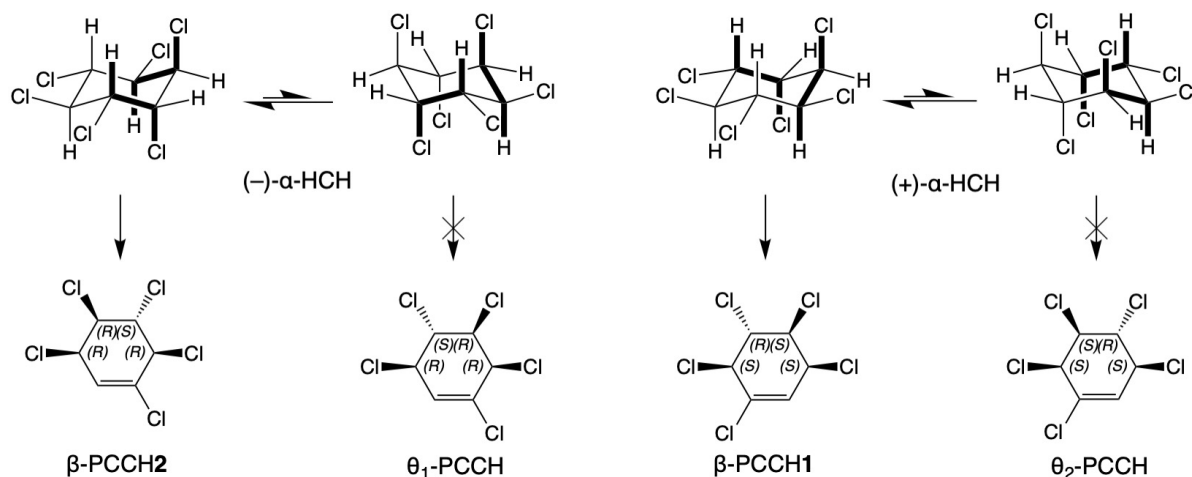


Figure S6 Possible PCCHs formed from different α -HCH enantiomers and conformers. From the two reactive positions in each conformer, marked bold, always the same PCCH is formed. We named the enantiomers according to their relative retention time on the γ -DEXTM 120 column as β -PCCH1 and β -PCCH2. θ -PCCHs were named according to the numbering used in Figure S5.

S5.5 Additional data for the LinA2 catalyzed transformation of β -HCH

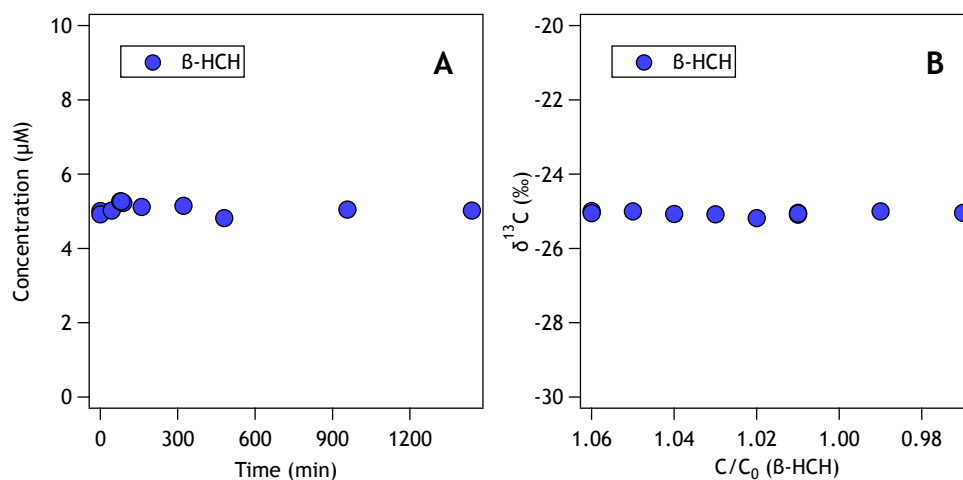


Figure S7 Absence of transformation of β -HCH in assays containing LinA2 illustrated by the constant substrate concentrations (panel A) and constant $\delta^{13}\text{C}$ values (panel B).

S5.6 Additional data for the LinB catalyzed transformation of β -HCH

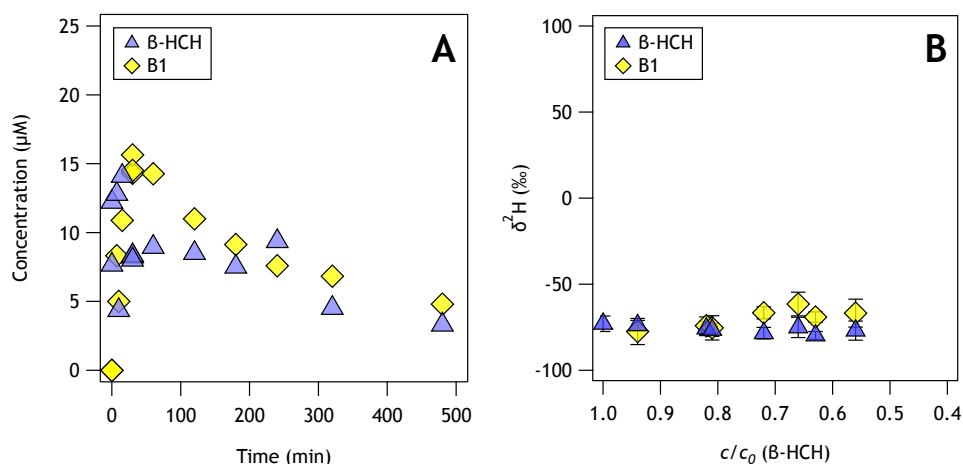


Figure S8 Panel A: Transformation of β -HCH to pentachlorocyclohexanol (B1) in batch reactors containing LinB at pH 7.5, with 25 μM nominal initial concentration. Panel B: Absence of H isotope fractionation during hydrolytic dechlorination of β -HCH to PCHL in experiment carried out with 6 μM nominal initial β -HCH concentration.

S6 References

- [1] Bala, K., Geueke, B., Miska, M. E., Rentsch, D., Poiger, T., Dadhwal, M., Lal, R., Holliger, C., and Kohler, H.-P. E. (2012). Enzymatic conversion of ϵ -hexachlorocyclohexane and a heptachlorocyclohexane isomer, two neglected components of technical hexachlorocyclohexane. *Environ. Sci. Technol.*, 46(7):4051–4058.
- [2] Bashir, S., Fischer, A., Nijenhuis, I., and Richnow, H.-H. (2013). Enantioselective carbon stable isotope fractionation of hexachlorocyclohexane during aerobic biodegradation by *Sphingobium* spp. *Environ. Sci. Technol.*, 47(20):11432–11439.
- [3] Bashir, S., Hitzfeld, K. L., Gehre, M., Richnow, H. H., and Fischer, A. (2015). Evaluating degradation of hexachlorocyclohexane (HCH) isomers within a contaminated aquifer using compound-specific stable carbon isotope analysis (CSIA). *Water Res.*, 71(0):187–196.
- [4] Chartrand, M., Passeport, E., Rose, C., Lacrampe-Couloume, G., Bidleman, T. F., Jantunen, L. M., and Sherwood Lollar, B. (2015). Compound specific isotope analysis of hexachlorocyclohexane isomers: a method for source fingerprinting and field investigation of in situ biodegradation. *Rapid Commun. Mass Spectrom.*, 29(6):505–514.
- [5] Dyballa, N. and Metzger, S. (2009). Fast and sensitive colloidal coomassie G-250 staining for proteins in polyacrylamide gels. *J. Vis. Exp.*, (30).
- [6] Geueke, B., Garg, N., Ghosh, S., Fleischmann, T., Holliger, C., Lal, R., and Kohler, H.-P. E. (2013). Metabolomics of hexachlorocyclohexane (HCH) transformation: ratio of lina to linb determines metabolic fate of HCH isomers. *Environ. Microbiol.*, 15(4):1040–1049.
- [7] Hoops, S., Sahle, S., Gauges, R., Lee, C., Pahle, J., Simus, N., Singhal, M., Xu, L., Mendes, P., and Kummer, U. (2006). COPASI - a complex pathway simulator. *Bioinformatics*, 22(24):3067–3074.
- [8] Kang, D., Gho, Y. S., Suh, M., and Kang, C. (2002). Highly sensitive and fast protein detection with coomassie brilliant blue in sodium dodecyl sulfate-polyacrylamide gel electrophoresis. *Bull. Korean Chem. Soc.*, 23(11):1511–1512.
- [9] Lal, R., Pandey, G., Sharma, P., Kumari, K., Malhotra, S., Pandey, R., Raina, V., Kohler, H.-P. E., Holliger, C., Jackson, C., and Oakeshott, J. G. (2010). Biochemistry of microbial degradation of hexachlorocyclohexane and prospects for bioremediation. *Microbiol. Mol. Biol. R.*, 74(1):58–80.
- [10] Liu, Y., Bashir, S., Stollberg, R., Trabitzzsch, R., Weiss, H., Paschke, H., Nijenhuis, I., and Richnow, H.-H. (2017). Compound specific and enantioselective stable isotope analysis as tools to monitor transformation of hexachlorocyclohexane (HCH) in a complex aquifer system. *Environ. Sci. Technol.*, 51(16):8909–8916.
- [11] Manna, R. N. and Dybala-Defratyka, A. (2013). Insights into the elimination mechanisms employed for the degradation of different hexachlorocyclohexane isomers using kinetic isotope effects and docking studies. *J. Phys. Org. Chem.*, 26(10):797–804.
- [12] Mössner, S. and Ballschmiter, K. (1994). Separation of α -hexachlorocyclohexane (α -hch) and pentachlorocyclohexene (pcch) enantiomers on a cyclodextrin phase (cyclodex-b) by hrgc/ecd. *Fresenius J. of Anal. Chem.*, 348(8-9):583–589.
- [13] Pati, S. G., Kohler, H.-P. E., and Hofstetter, T. B. (2017). Chapter eleven - characterization of substrate, cosubstrate, and product isotope effects associated with enzymatic oxygenations of organic compounds based on compound-specific isotope analysis. In Harris, M. E. and Anderson, V. E., editors, *Measurement and Analysis of Kinetic Isotope Effects*, volume 596 of *Methods in Enzymology*, pages 291–329. Academic Press.
- [14] Raina, V., Hauser, A., Buser, H. R., Rentsch, D., Sharma, P., Lal, R., Holliger, C., Poiger, T., Müller, M. D., and Kohler, H.-P. E. (2007). Hydroxylated metabolites of β - and δ -hexachlorocyclohexane: Bacterial formation, stereochemical configuration, and occurrence in groundwater at a former production site. *Environ. Sci. Technol.*, 41(12):4292–4298.
- [15] Raina, V., Rentsch, D., Geiger, T., Sharma, P., Buser, H. R., Holliger, C., Lal, R., and Kohler, H.-P. E. (2008). New metabolites in the degradation of α - and γ -hexachlorocyclohexane (HCH): pentachlorocyclohexenes are hydroxylated to cyclohexenols and cyclohexenediols by the haloalkane dehalogenase LinB from *Sphingobium indicum* B90A. *J. Agric. Food Chem.*, 56(15):6594–6603.
- [16] Reichert, P. (1994). Aquasim – a tool for simulation and data analysis of aquatic systems. *Water Sci. Technol.*, 30(2):21–30.
- [17] Schilling, I., Hess, R., Rup, L., Hofstetter, T. B., and E, K. H.-P. (2019). Kinetic isotope effects of the enzymatic transformation of γ -hexachlorocyclohexane by the lindane dehydrochlorinase variants LinA1 and LinA2. *Environ. Sci. Technol.*, in press, doi:10.1021/acs.est.8b04234.
- [18] Schimmelmann, A., Qi, H., Coplen, T. B., Brand, W. A., Fong, J., Meier-Augenstein, W., Kemp, H. F., Toman, B., Ackermann, A., Assonov, S., Aerts-Bijma, A. T., Brejcha, R., Chikaraishi, Y., Darwish, T., Elsner, M., Gehre, M., Geilmann, H., Groening, M., Helie, J.-F., Herrero-Martin, S., Meijer, H. A. J., Sauer, P. E., Sessions, A. L., and Werner, R. A. (2016). Organic reference materials for hydrogen, carbon, and nitrogen stable isotope-ratio measurements: Caffeines, n-alkanes, fatty acid methyl esters, glycines, l-valines, polyethylenes, and oils. *Anal. Chem.*, 88(8):4294–4302.
- [19] Shrivastava, N., Macwan, A. S., Kohler, H.-P. E., and Kumar, A. (2017). Important amino acid residues of hexachlorocyclohexane dehydrochlorinases ((lina)) for enantioselective transformation of hexachlorocyclohexane isomers. *Biodegradation*, 28(2-3):171–180.
- [20] Suar, M., Hauser, A., Poiger, T., Buser, H.-R., Müller, M. D., Dogra, C., Raina, V., Holliger, C., van der Meer, J. R., Lal, R., and Kohler, H.-P. E. (2005). Enantioselective transformation of α -hexachlorocyclohexane by the dehydrochlorinases LinA1 and LinA2 from the soil bacterium *Sphingomonas paucimobilis* B90A. *Appl. Environ. Microbiol.*, 71(12):8514–8518.
- [21] Trantirek, L., Hynkova, K., Nagata, Y., Murzin, A., Ansorgova, A., Sklenar, V., and Damborsky, J. (2001). Reaction mechanism and stereochemistry of γ -hexachlorocyclohexane dehydrochlorinase LinA. *J. Biol. Chem.*, 276(11):7734–7740.
- [22] Zhang, N., Bashir, S., Qin, J., Schindelka, J., Fischer, A., Nijenhuis, I., Herrmann, H., Wick, L. Y., and Richnow, H. H. (2014). Compound-specific stable isotope analysis (CSIA) to characterize transformation mechanisms of α -hexachlorocyclohexane. *J. Hazard. Mater.*, 280(0):750–757.